

## Host compatibility rather than vector–host-encounter rate determines the host range of avian *Plasmodium* parasites

Matthew C. I. Medeiros, Gabriel L. Hamer and Robert E. Ricklefs

*Proc. R. Soc. B* 2013 **280**, 20122947, published 17 April 2013

---

### Supplementary data

["Data Supplement"](#)

<http://rspb.royalsocietypublishing.org/content/suppl/2013/04/11/rspb.2012.2947.DC1.html>

### References

[This article cites 65 articles, 20 of which can be accessed free](#)

<http://rspb.royalsocietypublishing.org/content/280/1760/20122947.full.html#ref-list-1>

### Subject collections

Articles on similar topics can be found in the following collections

[ecology](#) (1403 articles)

### Email alerting service

Receive free email alerts when new articles cite this article - sign up in the box at the top right-hand corner of the article or click [here](#)



CrossMark  
click for updates

## Research

**Cite this article:** Medeiros MCI, Hamer GL, Ricklefs RE. 2013 Host compatibility rather than vector–host-encounter rate determines the host range of avian *Plasmodium* parasites. *Proc R Soc B* 280: 20122947. <http://dx.doi.org/10.1098/rspb.2012.2947>

Received: 10 December 2012

Accepted: 22 March 2013

### Subject Areas:

ecology

### Keywords:

avian malaria, *Plasmodium*, host-encounter rate, host compatibility, mosquito-feeding patterns, host range

### Author for correspondence:

Matthew C. I. Medeiros  
e-mail: [mcmn92@umsl.edu](mailto:mcmn92@umsl.edu)

Electronic supplementary material is available at <http://dx.doi.org/10.1098/rspb.2012.2947> or via <http://rspb.royalsocietypublishing.org>.

# Host compatibility rather than vector–host-encounter rate determines the host range of avian *Plasmodium* parasites

Matthew C. I. Medeiros<sup>1</sup>, Gabriel L. Hamer<sup>2,3</sup> and Robert E. Ricklefs<sup>1</sup>

<sup>1</sup>Department of Biology, University of Missouri–St Louis, One University Boulevard, St Louis, MO 63121-4499, USA

<sup>2</sup>Department of Microbiology and Molecular Genetics, Michigan State University, East Lansing, MI 48824, USA

<sup>3</sup>Department of Entomology, Texas A&M University, College Station, TX 77843-2475, USA

Blood-feeding arthropod vectors are responsible for transmitting many parasites between vertebrate hosts. While arthropod vectors often feed on limited subsets of potential host species, little is known about the extent to which this influences the distribution of vector-borne parasites in some systems. Here, we test the hypothesis that different vector species structure parasite–host relationships by restricting access of certain parasites to a subset of available hosts. Specifically, we investigate how the feeding patterns of *Culex* mosquito vectors relate to distributions of avian malaria parasites among hosts in suburban Chicago, IL, USA. We show that *Plasmodium* lineages, defined by cytochrome *b* haplotypes, are heterogeneously distributed across avian hosts. However, the feeding patterns of the dominant vectors (*Culex restuans* and *Culex pipiens*) are similar across these hosts, and do not explain the distributions of *Plasmodium* parasites. Phylogenetic similarity of avian hosts predicts similarity in their *Plasmodium* parasites. This effect was driven primarily by the general association of *Plasmodium* parasites with particular host superfamilies. Our results suggest that a mosquito-imposed encounter rate does not limit the distribution of avian *Plasmodium* parasites across hosts. This implies that compatibility between parasites and their avian hosts structure *Plasmodium* host range.

## 1. Introduction

Parasites are heterogeneously distributed across hosts [1]. This heterogeneity in host distribution can arise owing to (i) variability in the frequency of encounters between hosts and parasites and (ii) the ability of parasites to invade and persist on the hosts they encounter [2]. Combes [2] described these ecological drivers of host distribution as the encounter and host compatibility filters, respectively. Assessing the relative strength of these filters is a fundamental step in determining mechanisms that govern the distribution of a parasite across hosts. Understanding factors that modulate host range is important because changes in these factors alter transmission dynamics [3–5] and introduce novel parasites to naive hosts, sometimes with devastating consequences [6].

Previous studies have empirically demonstrated that both the encounter and host compatibility filter can be important obstacles for host infection. Studies commonly assess the strength of these filters by controlling for the encounter filter through experimental infection. These demonstrate that parasites differ in their compatibility with hosts [7–9], and that many are capable of infecting hosts outside their natural host range [10]. Infection probabilities on novel hosts can increase with phylogenetic relatedness with the original host, suggesting that the compatibility filter strengthens with increasing host phylogenetic distance [9,10]. Measuring the encounter filter directly in nature can be logistically difficult; however, studies that have done so reveal interesting patterns. Strong encounter filters can mask the influence of the host compatibility filter if less susceptible host species experience more encounters with parasites [11]. Strong encounter filters can exist in spite of high host–parasite sympatry. Non-parasitized host

species can occur in close proximity to highly parasitized host species [12], suggesting fine-tuning in the mechanisms of parasites to encounter hosts, and of hosts to evade them.

Vectors control host encounters for a diversity of parasites and provide a convenient way to measure encounter rates in nature. Many arthropod vectors transmit parasites between vertebrate hosts during blood-feeding activities. Thus, blood-feeding patterns effectively set the encounter rate between vector-borne parasites and hosts. Mosquitoes, which are important vectors for a diversity of pathogens, are known to feed heterogeneously across hosts by using some species disproportionately, relative to their abundance [13–15]. This heterogeneity in mosquito-feeding patterns can strongly influence disease transmission dynamics [3,4,13,16]. Mosquito-feeding networks may also be compartmentalized [17], with certain vector species using a distinct subset of available host species [14,18–21]. For instance, in the northeastern United States, *Culex restuans*, *Culex pipiens*, and *Culiseta melanura* obtain blood meals from birds, while the sympatric *Aedes vexans*, *Ochlerotatus* and *Anopheles* species rely primarily on mammals for blood meals [18,22,23].

Compartmentalization in vector-feeding patterns across hosts may serve as an ecological barrier to transmission, and limit access of vector-borne parasites to different suites of hosts [20]. In a community of hosts, vectors and vector-borne parasites, vector species can impose a limiting encounter filter for parasites by feeding on non-overlapping or weakly overlapping subsets of potential hosts [20,24]. These subsets form compartments in an interaction network that summarizes the feeding patterns of vectors on host species. If this network defines the routes parasites take to move between hosts, parasites would move more readily between hosts that exist within a compartment than between hosts that occupy different compartments. Accordingly, this would tend to homogenize parasite assemblages across host species that share the same compartments in the mosquito–host network. This model suggests an easily testable hypothesis, namely that host species fed upon by the same vector species harbour the same parasite species.

Avian malaria parasites of the genus *Plasmodium* provide a suitable system to investigate the impact of vector-feeding behaviour in delimiting the host range of a parasite. Avian *Plasmodium* parasites have complex life cycles, which include asexual stages of reproduction in a bird host and sexual stages of reproduction within a mosquito vector [25]. Briefly, the life cycle within the mosquito begins when gametocytes from an infectious bird are ingested during a blood meal. These gametocytes differentiate into gametes that fuse to form ookinetes in the mosquito midgut. Ookinetes develop into oocysts that attach to the midgut wall. Sporozoites develop within oocysts. Once released, they selectively invade the mosquito's salivary glands. Successful transmission between birds occurs when a mosquito survives long enough for the parasite to proceed through this life cycle and injects sporozoites into another bird upon taking a subsequent blood meal.

Despite the potential importance of vectors in structuring *Plasmodium*–host relationships, most studies have focused on characterizing the diversity of *Plasmodium* infections in avian hosts [26–32]. The identification of the vectors in these systems has lagged behind (but see [21,24,33–36]). Even fewer studies have investigated the role of vectors in the transmission process and in the evolutionary biology of these

parasites (but see [21,24,37,38]). However, many studies hypothesize that vector dynamics may explain distributional patterns of these parasites [21,37,39,40].

Patterns of avian *Plasmodium* host range are highly idiosyncratic [26–29,38,41]. *Plasmodium* parasites are non-randomly distributed across host species, typically infecting only a subset of available hosts [26,28]. Some avian *Plasmodium* taxa are nearly restricted to a single host species [29,32]. In addition, these relationships can vary geographically, and *Plasmodium* parasites may occur on different hosts across their range [28,41]. These host–parasite relationships are not well preserved through time [42], and co-phylogenetic analyses of parasites and hosts reveal that host switching over evolutionary time-scales is pervasive [43,44]. These geographically variable relationships and host-switching events suggest that avian *Plasmodium* parasites have the ability to evolve the necessary machinery to exploit a broad range of hosts, despite their restricted host ranges at any given point in space and time. This raises the possibility that an encounter filter imposed by modular mosquito-feeding patterns could account for this apparent contradiction, by restricting access to only a subset of hosts that can be exploited by an avian *Plasmodium* parasite [24].

The topic has been approached before within the avian *Plasmodium* system. Gager *et al.* [24] integrated information on the distribution of *Plasmodium* lineages across vectors and the avian host *Turdus grayi* in central Panama. They discovered that two common *Plasmodium* lineages of *T. grayi* occurred in different vector species, demonstrating that the two species of vectors feed on *T. grayi*. In addition, the vectors carried many *Plasmodium* lineages that were not isolated from *T. grayi* despite access to this host. The study did not support the existence of a limiting encounter filter because *T. grayi* were exposed to both vectors and all the avian malaria lineages in the study area, but only a subset of *Plasmodium* lineages were found to infect *T. grayi* individuals. However, the study was limited to a single avian host, did not resolve the feeding patterns of vectors, and did not explore the hypothesis in a community context.

Here, we evaluate the influence of mosquito vectors in modulating the distribution of specific *Plasmodium* taxa across a community of avian hosts in suburban Chicago, IL, USA. Specifically, we identify local avian *Plasmodium* vectors and use a series of analyses to investigate whether their feeding patterns influence how *Plasmodium* parasites are distributed across avian hosts. We also investigate the potential for host compatibility to structure these relationships. Cumulatively, we assess the relative strength of a mosquito-imposed encounter filter and compatibility filter in delimiting the distribution of avian *Plasmodium* parasites across a host community in an effort to understand factors that influence parasite host range. We find mosquito-feeding patterns do not explain the heterogeneous distributions of *Plasmodium* parasites across avian hosts, suggesting that host compatibility issues dominate processes that structure parasite host range in this system.

## 2. Material and methods

### (a) Study system and sampling

The study was conducted in 17 scattered suburban sites including parks, cemeteries and residential communities in Chicago, IL, USA ([45]; <http://www.vetmed.wisc.edu/WNV>). Avian blood samples

were collected from May through to September during 2006 and 2007. Mosquito samples were collected with canopy-level Centres of Disease Control light traps [46] from June through to September during the same years at 13 of the 17 sites in which birds were captured.

### (b) Resolving mosquito-feeding patterns

Mosquito-feeding patterns were resolved by Hamer *et al.* [14]. The study identified the vertebrate source of 1043 blood meals of nine mosquito species in suburban Chicago. Six of the mosquito species were observed to feed on birds. However, only *C. pipiens*, *C. restuans* and *A. vexans* were well sampled, fed on birds and were abundant within the study area [46]. Avian blood meals were recovered from 488 *C. pipiens*, 172 *C. restuans* and 15 *A. vexans* individuals sampled from 2005 to 2007. An additional 75 *C. pipiens* and 77 *C. restuans* from 2008 to 2009 were added to the analysis presented here. Molecular procedures for identifying *Culex* blood meals may be found in Hamer *et al.* [14]. Engorged mosquitoes were sampled in the same study sites at which both avian hosts and mosquito vectors were surveyed for parasites. While *C. pipiens* represents a well-known species complex, previous study showed that introgression of *molestus* and *quiquefasciatus* forms is minimal in the Chicago population [47]. Thus, the numerous behavioural and physiological differences between these forms [48] are unlikely to influence the patterns presented here.

### (c) Resolving parasite–bird and parasite–mosquito relationships

Avian hosts were sampled using standard mist netting protocols. Blood was obtained by jugular venepuncture and was stored in BA-1 diluent or Longmire's lysis buffer at less than  $-20^{\circ}\text{C}$ . A subsample of 10  $\mu\text{l}$  was used to extract DNA using an ammonium acetate protein precipitation procedure. Samples were purified through a standard isopropanol precipitation followed by two consecutive washes with 70 per cent ethanol. Samples were eluted in double-distilled polymerase chain reaction (PCR)-grade water for at least 3 days before further processing. DNA samples were screened for the presence of haemosporidian parasites through a PCR that targeted a small segment of the 16S rRNA gene [49]. Samples that screened positive with the 16S rRNA primers were used in a secondary nested PCR that targeted a 552 bp fragment of the haemosporidian cytochrome *b* gene. Details of this reaction are presented by Fecchio *et al.* [50]. The fragment was sequenced to identify the haemosporidian responsible for the infection.

The taxonomy of avian Haemosporida is controversial and currently unresolved. Traditionally, subtle morphological characters were used to distinguish taxa [25]. However, recent studies have demonstrated substantial genetic diversity within some morphospecies, and have raised the possibility of cryptic species in this system [31,51–53]. However, the status of most haemosporidian parasites as biological species remains untested. Thus, no species level of genetic divergence can be established. In addition, reliable independent nuclear markers are not available to identify isolated lineages by linkage disequilibrium criteria [51]. Here, we delimit evolutionary-independent parasite lineages based on the similarity of cytochrome *b* haplotypes in a manner similar to Ricklefs *et al.* [29]. Evolutionary-independent lineages are defined as the set of closely related (less than 1% sequence divergence) monophyletic parasite mitochondrial haplotypes recovered from the same host species or set of host species. Cytochrome *b* haplotypes of *Plasmodium* lineages identified in this manuscript are deposited in GenBank (accession no. KC789821–KC789828).

Three mosquito species (*A. vexans*, *C. pipiens*, and *C. restuans*) that were abundant [46] and observed to feed on birds in Chicago [14] were screened for the presence of *Plasmodium* parasites. Previous research has demonstrated that these *Culex* species are

known avian malaria vectors [25] and are infected with many of the same avian *Plasmodium* lineages [36]. Little information exists on the vectorial capacity of *A. vexans*. This species was included in this parasite survey because it fed on birds and was abundant in the study site [46]. Individuals were pooled by species, site and date of capture. Pool sizes varied from 1 to 36 whole-bodied individuals. *Culex pipiens* and *C. restuans* are not reliably distinguished based on morphology [54]. Owing to the time and expense of the molecular diagnostics to distinguish these species [55], the *Culex* species were pooled together. DNA was extracted from mosquito pools using Qiagen blood and tissue kits following the manufacturer's protocol. Mosquito DNA samples were screened and haemosporidian infections were identified using the same molecular procedures for bird hosts. Maximum-likelihood estimates of the infection rate in mosquitoes were calculated with the POOLINF RATE (www.cdc.gov), v. 4.0 add-in for Microsoft EXCEL [56].

Because whole-bodied mosquitoes were used, we cannot distinguish the proportion of mosquitoes that had infectious sporozoites, which typically occupy the salivary glands in the thorax, from those that had ookinete or oocysts infections within the midgut [25]. We assume that the proportion of infected mosquitoes is correlated with the proportion of infectious mosquitoes across different *Plasmodium* lineages. This assumption is supported by Ishtiaq *et al.* [33], who demonstrated that *Plasmodium* prevalence from mosquito thorax isolations was statistically indistinguishable from abdominal isolations in wild mosquitoes collected across southwest Pacific Islands.

### (d) Host phylogenetic distance estimates

Phylogenetic distances between hosts were estimated with a phylogenetic tree based on a 656 bp fragment of the recombination-activating gene 1 (RAG1). A maximum-likelihood gene tree was constructed using the PHYML plug-in in the program GENEIOUS [57]. The resulting topology was similar to that of Barker *et al.* [58]. See the electronic supplementary material, §2 for more information. Novel RAG1 sequences obtained for this study are deposited in GenBank (accession no. KC789829–KC789833).

### (e) Statistical analyses

All analyses performed here focus on 10 commonly sampled avian host species with seven or more infections of one or more of seven commonly sampled *Plasmodium* lineages (summarized in table 1). Two *Plasmodium* cytochrome *b* haplotypes were identical to those of known *Plasmodium* morphospecies: *Plasmodium cathemerium* (AY377128, [59]) and *Plasmodium elongatum* (AY733088, [60]). These lineages are referred to by their scientific name. The mosquito-feeding patterns of the two *Culex* species across the 10 common avian *Plasmodium* hosts were compared with a G-test. One was added to each cell to avoid problems associated with zero cell values.

Mantel tests were used to assess whether (i) pairwise similarities in relationships between hosts and mosquitoes inferred from the blood-feeding patterns, and (ii) phylogenetic distance between host species were associated with pairwise similarity in the distribution of *Plasmodium* parasites across all pairwise combinations of host species. This statistical test measures the correlation between two equivalent distance matrices and assesses significance through a process of permutation. Each matrix used in the two Mantel tests placed the seven host species along rows and columns. The Morisita–Horn quantitative similarity index was used to estimate similarity in both the relationships with mosquitoes and *Plasmodium* parasites between host pairs. The Morisita–Horn quantitative similarity index was chosen because it best handled variation in the number of identified *Plasmodium* infections between hosts involved in a comparison. Morisita–Horn distances were computed using the *vegan* package in program R. Phylogenetic distance between host pairs was based on

**Table 1.** Number of *Plasmodium* infections of specific lineages across all 10 avian hosts and *Culex* mosquito vectors. (MLE<sub>α</sub> is a bias-corrected maximum-likelihood estimate of the number of infected mosquitoes per 1000 individuals for each *Plasmodium* lineage. Upper and lower 95% confidence limits are shown within parentheses. Abbreviations for host species include the first letter of the genus, and the first two letters of the species name respectively. APH, *Agelaius phoeniceus* (red-winged blackbird); CCA, *Cardinalis cardinalis* (northern cardinal); CME, *Carpodacus mexicanus* (house finch); DCA, *Dumetella carolinensis* (grey catbird); MAT, *Molothrus ater* (brown-headed cowbird); MME, *Melospiza melodia* (song sparrow); PDO, *Passer domesticus* (house sparrow); QQU, *Quiscalus quiscula* (common grackle); SVU, *Sturnus vulgaris*, (European starling); TMI, *Turdus migratorius* (American robin).)

<i>Plasmodium</i> parasites								
	CHI02PL	CHI04PL	CHI07PL	CHI09PL	<i>P. CATH</i>	<i>P. ELON</i>	CHI05PL	total
hosts								
APH	0	0	0	0	4	2	1	7
CCA	0	0	0	0	26	24	2	52
CME	0	0	0	0	4	12	0	16
DCA	0	2	4	0	4	10	0	20
MAT	0	0	0	0	3	7	0	10
MME	0	0	0	0	11	6	3	20
PDO	0	0	2	1	56	17	20	96
SVU	0	0	6	0	7	0	0	13
TMI	35	23	144	9	9	5	2	227
QQU	0	0	0	0	10	2	0	12
total	35	25	156	10	134	85	28	
vectors								
CULEX	14	37	29	2	32	12	2	128
MLE <sub>α</sub>	2.3	6.35	4.7	0.32	5.3	2.0	0.32	
	(1.3, 3.8)	(4.6, 8.7)	(3.2, 6.8)	(0.06, 1.1)	(3.6, 7.4)	(1.1, 3.3)	(0.06, 1.1)	

phylogenetic branch lengths (see the electronic supplementary material, §2). Results did not change when per cent sequence divergence was used instead of patristic distances. For both Mantel tests, a significance test of the association between the matrices was based on 10 000 randomized permutations. Mantel tests were performed in program R using the *vegan* package.

Similarity between parasite assemblages was visualized using non-metric multidimensional scaling (NMDS). The number of dimensions was determined by the elbow test based on the relationship between the stress of an individual ordination and the number of dimensions. Stress is the proportion of the residual sum of squares of the deviations from a monotonic regression of observed on predicted distances of species in ordination space. There was a dramatic reduction in stress (0.002 to less than 0.0001), between ordinations with two and three dimensions in the analysis with a marginal reduction (less than 0.0001) between three and four dimensions. Thus, three dimensions were used in the analysis. Pair-wise similarities between parasite assemblages on host species and the mosquito vectors were compared statistically using *G*-tests. All *G*-tests were conducted in Microsoft EXCEL using the pop tools v. 3.2.5 add-in (<http://www.poptools.org>).

A Monte Carlo approach was used to simulate the distributions of each *Plasmodium* lineage across host species. Three separate simulations were performed, each with a unique set of assumptions (see the electronic supplementary material, §S3). All simulations were run in program R, using the function 'rmultinom' to generate multinomially distributed random number vectors based on a specified probability distribution. The expected value (the mean of the simulated values) and the 5% confidence limits for each *Plasmodium*–host pair were extracted from the vectors. More information is presented in the electronic supplementary material, §3.

### 3. Results

All seven common *Plasmodium* lineages recovered from avian hosts were discovered in *Culex* mosquito pools. Maximum-likelihood estimates of mosquito infection rates for each *Plasmodium* lineage are presented in table 1. *Plasmodium* parasites were not detected among *A. vexans* pools. The mosquito-feeding patterns and the parasite screening results suggest *C. pipiens* and *C. restuans* are the major *Plasmodium* vectors in Chicago. Thus, *A. vexans* was not included in subsequent analyses.

Patterns of avian host use did not differ significantly between of *C. restuans* and *C. pipiens* (figures 1, 2;  $G = 14.7$ , d.f. = 9,  $p = 0.10$ , electronic supplementary material, table S1), suggesting that the two main vector species interact with a similar set of avian *Plasmodium* hosts. A Mantel test revealed no significant correlation between similarities in relationships with avian *Plasmodium* vectors and *Plasmodium* lineages across avian hosts ( $r = -0.09$ ,  $p = 0.58$ ), suggesting that host interactions with *Plasmodium* are not structured by the limited (and insignificant) variation in host utilization by mosquito vectors. This result remained unchanged when considering infections from hatch-year or after hatch-year birds independently (see the electronic supplementary material, §4).

By contrast, relationships between avian host species and *Plasmodium* lineages were strikingly heterogeneous (table 1;  $G = 411$ , d.f. = 54,  $p < 0.001$ ). NMDS demonstrated relationships between *Plasmodium* lineages, avian hosts and *Culex* vectors (figure 2). The ordination split hosts and parasites into two groups. Host species within the superfamily

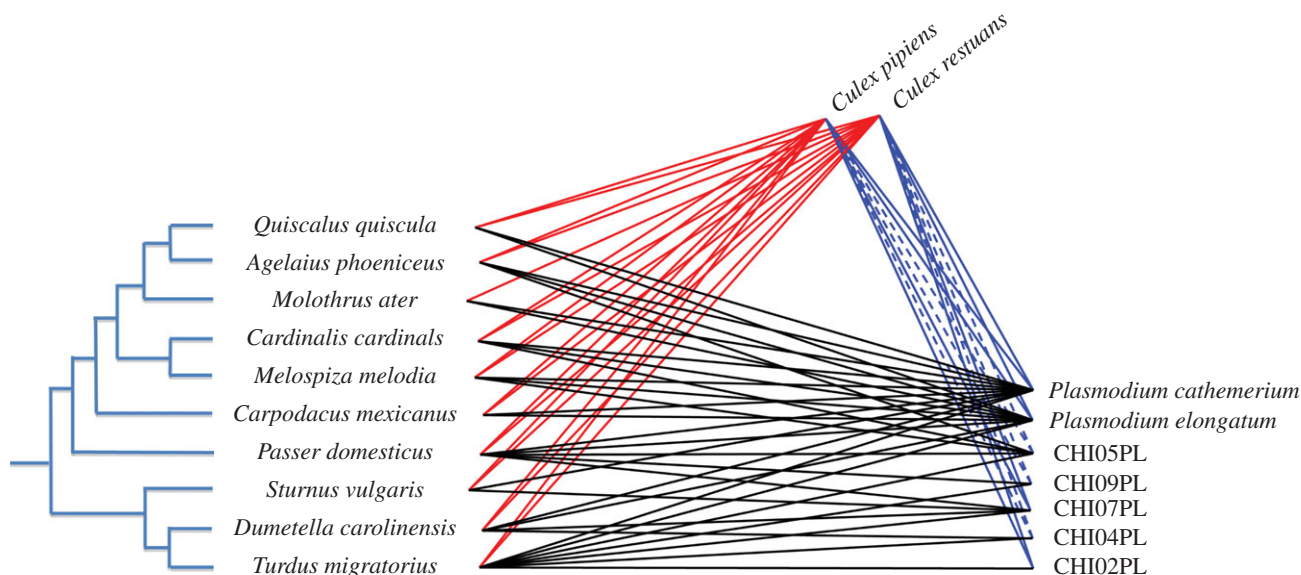


**Figure 1.** A tripartite interaction network demonstrating the relationships between avian hosts, *Culex* vectors and *Plasmodium* parasites in Chicago, IL, USA. The topology of the host phylogenetic tree was based on a maximum-likelihood analysis of RAG1 (see the electronic supplementary material). Connections between host and parasite, and host and vector are based on the parasite screening results presented here, and vector blood meal analyses presented in Hamer *et al.* [14]. Connections between mosquito vectors and parasites denoted by solid lines are based on published accounts of vectorial capacity (summarized in Valkiūnas [25]) or documented infections that were naturally acquired in those mosquito species (Kimura *et al.* [36]). Connections denoted by dashed lines are not reported in either Valkiūnas [25] or Kimura *et al.* [36], but instead are inferred from data presented here where exact species-level interactions cannot be determined owing to mixed *Culex* mosquito pools. (Online version in colour.)

Muscicapoidea (*Turdus migratorius*, *Sturnus vulgaris*, *Dumetella carolinensis*) overlap with the parasite lineages CHI02PL, CHI04PL, CHI07PL and CHI09PL, whereas those within the superfamily Passeroidea (*Agelaius phoeniceus*, *Cardinalis cardinals*, *Carpodacus mexicanus*, *Melospiza melodia*, *Molothrus ater*, *Passer domesticus*, *Quiscalus quiscula*) group with *P. cathemerium*, *P. elongatum*, and CHI05PL. A Mantel test revealed a positive correlation (Mantel  $r = 0.58$ ,  $p = 0.006$ ) between phylogenetic similarity as indicated by branch lengths separating host species (see the electronic supplementary material, table S2) and the similarity of parasite relationships between host species pairs. The *Plasmodium* assemblage on *Culex* vectors grouped within the Muscicapoidea cluster. CHI02PL, CHI04PL, CHI07PL and CHI09PL composed 64 per cent of the *Plasmodium* parasites in *Culex* vectors. *Plasmodium cathemerium*, *P. elongatum*, and CHI05PL composed 36 per cent of that parasite assemblage.

Pairwise *G*-tests offered a statistically explicit approach to assessing differences in *Plasmodium* assemblages across hosts and vectors. The tests, summarized in electronic supplementary material, figure S1, demonstrate that the *Plasmodium* assemblage of *T. migratorius* differed significantly from all other assemblages. This is associated with the high degree of association between *T. migratorius* and four of seven common *Plasmodium* lineages. Seven other pairwise comparisons differed significantly. Five of these pairs compared assemblages of Muscicapoidea and Passeroidea hosts. Excluding *T. migratorius*, all comparisons between host pairs within Muscicapoidea or the nine-primaried New World Passeroidea (all Passeroidea host here except *P. domesticus*) were statistically indistinguishable. Interestingly, eight of 10 comparisons between the *Plasmodium*

assemblages on vectors and those of avian hosts exhibited significant differences.

Three separate Monte Carlo simulations, each with a unique set of assumptions (see the electronic supplementary material, §S3), revealed patterns consistent with the other analyses. The simulations suggest *T. migratorius* have more CHI02PL, CHI04PL and CHI07PL infections and less *P. elongatum*, *P. cathemerium*, and CHI05PL infections than expected (see the electronic supplementary material, tables S3a–e). Well-sampled Passeroidea hosts showed the opposite pattern. See electronic supplementary material, §3 for more information.

## 4. Discussion

Our original model of a limiting host-encounter filter for vector-borne parasites hinged on a key assumption: vectors feed on different subsets of hosts and these divergent feeding patterns structure parasite assemblages on hosts. This assumption was not supported by any of our analyses. Feeding patterns of the two dominant avian *Plasmodium* vectors were similar, highly connected, and provided different *Plasmodium* lineages the same relative access across host species. Moreover, the limited variation in the feeding patterns between *C. restuans* and *C. pipiens* did not explain variation in *Plasmodium* assemblages across hosts. Our data demonstrate that the feeding patterns of *Culex* mosquitoes in Chicago, IL, do not impose a compartmentalized encounter filter that structures the relationships between *Plasmodium* taxa and common avian host species.

Assemblages of *Plasmodium* parasites on avian host species were heterogeneous despite the similar feeding patterns of the two *Culex* species. This strongly suggests that compatibility

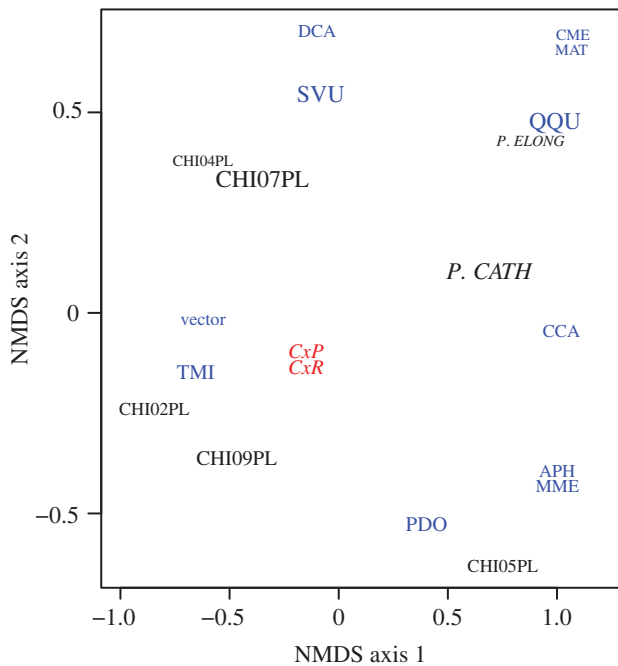


**Figure 2.** Plot demonstrating the results of a three-dimensional NMDS ordination of parasite–host relationships. The font size of the text is directly proportional to the value in the third dimension. The three letter abbreviations for hosts include the first letter of the genus name and first two letters of the species name in that order. ‘Vector’ represents the assemblage of parasites found in positive *Culex* pools. The proximity of hosts in this three-dimensional ordination space demonstrates similarity in their parasite assemblages. The relative positions of the parasites in this three-dimensional ordination space graphically demonstrate the composition of these assemblages. CxP and CxR represent the distribution of blood meals for *Culex pipiens* and *Culex restuans*, respectively. These points were calculated as  $\sum p_i \text{NMDS}1_i + p_i \text{NMDS}2_i + p_i \text{NMDS}3_i$  where  $p_i$  is the proportion of blood meals of host species  $i$  for a mosquito species and  $\text{NMDS}x_i$  is the  $x$ -dimension NMDS score of host species  $i$ . These points are centrally located between all potential host species and overlap significantly, suggesting broad and similar feeding patterns between the two *Culex* species. Refer to table 1 for the genus and species explanations. (Online version in colour.)

issues that exist solely between the host and parasite structure these *Plasmodium*–bird relationships. This is corroborated by three important results of our analyses. (i) Significant differences exist between the *Plasmodium* assemblage on mosquito vectors and eight of 10 of the *Plasmodium* assemblages on hosts. In the absence of compartmentalized vector-feeding patterns, these differences must arise from differential compatibilities between host and parasite pairs. (ii) Monte Carlo simulations demonstrate that the frequency of infections of particular lineages in specific host species deviate from expectations. These comparisons reveal the presence of specific compatibility filters. (iii) Both the NMDS ordination and a Mantel test revealed that host relationships with *Plasmodium* parasites are phylogenetically structured in this system. Like other studies [9,10], this suggests that the compatibility filter strengthens with increasing phylogenetic distance.

Specific examples of both strong and porous host compatibility filters were evident within our data. Many hosts had fewer infections of specific *Plasmodium* lineages than expected by random assortment of hosts and parasites or the relative access provided by mosquito vectors. For instance, CHI02PL, CHI04PL and CHI07PL were absent to rare in Passeroidea hosts despite these lineages making up 64 per cent of the infections in vectors. Perhaps the most striking example

of parasite–host incompatibility is the near absence of *P. elongatum* and *P. cathemerium* from *T. migratorius*, despite these parasites being common in *Culex* mosquitoes, and the high frequency of contact between *T. migratorius* and these vectors. The apparent cases of incompatibility may arise through two distinct mechanisms. These *Plasmodium* lineages may have high virulence on these host species, and increase the probability of mortality before sampling [61]. Alternatively, these hosts may be resistant to the infection. This could be owing to adaptations of the immune system (such as those associated with major histocompatibility complex [62–64] or host cell surface proteins [65]), the lack of necessary machinery of the parasite to invade and persist in certain hosts, or both. Palinauskas *et al.* [7] demonstrated that experimentally challenged host species differed in their level of resistance towards *Plasmodium relictum*. Ultimately, experimental infection studies like this are necessary to discriminate between these hypotheses.

In addition, some *Plasmodium* lineages were more frequent in specific hosts than expected. *Plasmodium cathemerium* and *P. elongatum* occurred more frequently in some Passeroidea hosts. CHI05PL was recovered disproportionately from *P. domesticus*. However, the most obvious example of this is the frequent recovery of CHI02PL, CHI04PL and CHI07PL from *T. migratorius*. These parasites were largely restricted to *T. migratorius*, and parasitized this host at rates that exceeded expectations generated by random association or the vector-imposed encounter rate. Indeed, our analyses suggest that CHI02PL, CHI04PL and CHI07PL may be specialized on *T. migratorius*. Specialization on *T. migratorius* may not be coincidental. This host species accounts for more than 60 per cent of the blood meals of both *Culex* vector species, making it the most encountered host in the community for mosquito-borne *Plasmodium* parasites. The high probability of encounter for these *Plasmodium* parasites with *T. migratorius* probably mitigates a primary cost of specialization: the failure to find optimal hosts because they are infrequent in a multi-host community [66].

Expansions in host range can result when changes in vector–host contact rates introduce parasites to novel hosts [17]. However, numerous studies have revealed an important interplay between host compatibility and the encounter rate in driving pathogen transmission dynamics over time [3], space [5] and between ecological communities that differ in structure [4,67]. Indeed, host range expansions also depend on the compatibility of novel hosts toward those parasites, and will not proceed if new host–parasite combinations are incompatible. Traits that influence host compatibility, and its constituent properties of host susceptibility, parasite infectivity, and the virulence of infection, evolve over time [68,69]. In the West Indies, the same suite of avian hosts and malaria parasites assemble into different patterns of relationships across island replicates [27,28,41], and there is some evidence that these differences can arise over short time periods [42]. If host compatibility issues outweigh heterogeneity in the encounter rate in structuring these parasite–host relationships, such idiosyncratic patterns observed in the West Indies and elsewhere may suggest that compatibility mechanisms are highly labile, even when parasites with complex life cycles are involved.

Fieldwork was carried out with permission from the Illinois Department of Works, and under animal-use approvals from the University of Illinois Animal Use Protocol no. 03034 and Institutional Animal Care and Use Committee at Michigan State University, Animal Use Form no. 12/03-152-00.

We thank the villages of Alsip, Evergreen Park, Oak Lawn and Palos Hills, and many private homeowners for granting us permission to conduct this study on their properties. Field assistance was provided by Scott Loss, Tim Thompson, Diane Gohde, Mike Goshorn and Seth Dallmann. Jon-Erik Hansen provided help processing samples in the laboratory. This manuscript was improved greatly by comments from A. Marm Kilpatrick, Patricia Baião and an anonymous reviewer, and discussions with Vincenzo Ellis, Maria Coelho-Svensson, Jenni Higashiguchi (*In memoriam*), Elliot Miller, Robert Marquis, Amy

Zanne and Patricia Parker. The collection of samples in Chicago, IL, was supported by the National Science Foundation grant no. EF-0429124 to Uriel D. Kitron, Jeffrey D. Brawn, Tony L. Goldberg, Marilyn O. Ruiz and Edward D. Walker. Sample processing and analysis was supported by the National Science Foundation grant no. DEB-054239, the Whitney Harris World Ecology Center, the St Louis Audubon Society, the Curators of the University of Missouri, and the University of Missouri–St Louis Dissertation Fellowship awarded to M.C.M. This publication is part of M.C.M.'s PhD dissertation.

## References

- Poulin R. 2007 *Evolutionary ecology of parasites*, 2nd edn. Princeton, NJ: Princeton University Press.
- Combes C. 1991 Evolution of parasite life cycles. In *Parasite–host associations: coexistence or conflict?* (eds C Toft, A Aeschlimann, L Bolis), pp. 62–82. Oxford, UK: Oxford University Press.
- Kilpatrick AM, Kramer LD, Jones MJ, Marra PP, Daszak P. 2006 West Nile virus epidemics in North America are driven by shifts in mosquito feeding behavior. *PLoS Biol* **4**, e82. (doi:10.1371/journal.pbio.0040082)
- Simpson JE, Hurtado PJ, Medlock J, Molaei G, Andreadis T, Galvani AP, Diuk-Wasser MA. 2012 Vector host-feeding preferences drive transmission of multi-host pathogens: West Nile virus as a model system. *Proc. R. Soc. B* **279**, 925–933. (doi:10.1098/rspb.2011.1282)
- Allan BF *et al.* 2010 Invasive honeysuckle eradication reduces tick-borne disease risk by altering host dynamics. *Proc. Natl Acad. Sci. USA* **107**, 18 523–18 527. (doi:10.1073/pnas.1008362107)
- van Riper C, van Riper SG, Goff ML, Laird M. 1986 The epizootiology and ecological significance of malaria in Hawaiian landbirds. *Ecol. Monogr.* **56**, 327–344. (doi:10.2307/1942550)
- Palinauskas V, Valkiūnas G, Bensch S, Bolshakov VC. 2008 Effects of *Plasmodium relictum* (lineage P-SGS1) on experimentally infected passerine birds. *Exp. Parasitol.* **120**, 372–380. (doi:10.1016/j.exppara.2008.09.001)
- Komar N, Langevin S, Hinten S, Nemeth N, Edwards E, Hettler D, Davis B, Bowen R, Bunning M. 2003 Experimental infection of North American birds with the New York 1999 strain of West Nile virus. *Emerg. Infect. Dis.* **9**, 311–322. (doi:10.3201/eid0903.020628)
- Gilbert GS, Webb CO. 2007 Phylogenetic signal in plant pathogen–host range. *Proc. Natl Acad. Sci. USA* **104**, 4979–4983. (doi:10.1073/pnas.0607968104)
- Pearlman SJ, Jaenike J. 2003 Infection success in novel hosts: an experiment and phylogenetic study of *Drosophila*–parasitic nematodes. *Evolution* **57**, 544–557.
- Detwiler JT, Minchella DJ. 2009 Intermediate host availability masks the strength of experimentally-derived colonization patterns in echinostome trematodes. *Int. J. Parasitol.* **39**, 585–590. (doi:10.1016/j.ijpara.2008.10.008)
- Kuris AM, Goddard JH, Torchin ME, Murphy N, Gurney R, Lafferty KD. 2007 An experimental evaluation of host specificity: the role of encounter and compatibility filters for a Rhizocephalan parasite of crabs. *Int. J. Parasitol.* **37**, 539–545. (doi:10.1016/j.ijpara.2006.12.003)
- Kilpatrick AM, Daszak P, Jones MJ, Marra PP, Kramer LD. 2006 Host heterogeneity dominates West Nile virus transmission. *Proc. R. Soc. B* **273**, 2327–2333. (doi:10.1098/rspb.2006.3575)
- Hamer GL, Kitron UD, Goldberg TL, Brawn JD, Loss SR, Ruiz MO, Hayes DB, Walker ED. 2009 Host selection by *Culex pipiens* mosquitoes and West Nile virus amplification. *Am. J. Trop. Med. Hyg.* **80**, 268–278.
- Hassan HK, Cupp EW, Hill GE, Katholi CR, Klingler K, Unnasch TR. 2003 Avian host preference by vectors of eastern equine encephalomyelitis virus. *Am. J. Trop. Med. Hyg.* **69**, 641–647.
- Hamer GL, Chaves LF, Anderson TK, Kitron UD, Brawn JD, Ruiz MO, Loss SR, Walker ED, Goldberg TL. 2011 Fine-scale variation in vector host use and force of infection drive localized patterns of West Nile virus transmission. *PLoS ONE* **6**, e23767. (doi:10.1371/journal.pone.0023767)
- Graham SP, Hassan HK, Burkett-Cadena N, Guyer C, Unnasch TR. 2009 Nestedness of ectoparasite–vertebrate host networks. *PLoS ONE* **4**, e7873. (doi:10.1371/journal.pone.0007873)
- Molaei G, Andreadis TG, Armstrong PM, Diuk-Wasser M. 2008 Host-feeding patterns of potential mosquito vectors in Connecticut, USA: molecular analysis of bloodmeals from 23 species of *Aedes*, *Anopheles*, *Culex*, *Coquillettidia*, *Psorophora*, and *Uranotaenia*. *J. Med. Entomol.* **45**, 1143–1151. (doi:10.1603/0022-2585(2008)45[1143:HPOPMV]2.0.CO;2)
- Malmqvist B, Strasevicius D, Hellgren O, Alder PH, Bensch S. 2004 Vertebrate host specificity of wild-caught blackflies revealed by mitochondrial DNA in blood. *Proc. R. Soc. Lond. B* **271**, S152–S155. (doi:10.1098/rsbl.2003.0120)
- Hellgren O, Bensch S, Malmqvist B. 2008 Bird hosts, blood parasites and their vectors: associations uncovered by molecular analyses of blackfly blood meals. *Mol. Ecol.* **17**, 1605–1613. (doi:10.1111/j.1365-294X.2007.03680.x)
- Kim KS, Tsuda Y. 2012 Avian *Plasmodium* lineages found in spot surveys of mosquitoes from 2007 to 2010 at Sakata wetland, Japan: do dominant lineages persist for multiple years? *Mol. Ecol.* **21**, 5374–5385. (doi:10.1111/mec.12047)
- Molaei G, Andreadis TG, Armstrong PM, Anderson JF, Vossbrinck CR. 2006 Host feeding patterns of *Culex* mosquitoes and West Nile virus transmission, Northeastern United States. *Emerg. Infect. Dis.* **12**, 468–474. (doi:10.3201/eid1203.051004)
- Molaei G, Oliver J, Andreadis TG, Armstrong PM, Howard JJ. 2006 Molecular identification of blood meal sources in *Culiseta melanura* and *Culiseta morsitans* from a focus of Eastern Equine Encephalomyelitis (EEE) virus transmission in New York, USA. *Am. J. Trop. Med. Hyg.* **75**, 1140–1147.
- Gager AB, Del Rosario Loaiza J, Dearborn DC, Bermingham E. 2008 Do mosquitoes filter the access of *Plasmodium* cytochrome *b* lineages to an avian host? *Mol. Ecol.* **17**, 2552–2561. (doi:10.1371/journal.pbio.0040082)
- Valkiūnas G. 2005 *Avian malaria parasites and other Haemosporidia*. Boca Raton, FL: CRC Press.
- Bensch S, Sijmen M, Hasselquist D, Östman Ö, Hansson B, Westerdaal H, Pinheiro RT. 2000 Host specificity in avian blood parasites: a study of *Plasmodium* and *Haemoproteus* mitochondrial DNA amplified from birds. *Proc. R. Soc. Lond. B* **267**, 1583–1589. (doi:10.1098/rspb.2000.1181)
- Fallon SM, Bermingham E, Ricklefs RE. 2003 Island and taxon effects in parasitism revisited: avian malaria in the Lesser Antilles. *Evolution* **57**, 606–615.
- Fallon SM, Bermingham E, Ricklefs RE. 2005 Host specialization and geographic localization of avian malaria parasites: a regional analysis in the Lesser Antilles. *Am. Nat.* **165**, 466–480. (doi:10.1086/428430)
- Ricklefs RE, Swanson BL, Fallon SM, Martinez-Abraín A, Scheuerlein A, Gray J, Latta SC. 2005 Community relationships of avian malaria parasites in southern Missouri. *Ecol. Monogr.* **75**, 543–559. (doi:10.1890/04-1820)
- Beadell JS, Gering E, Austin J, Dumbacher JP, Pierce MA, Pratt TK, Atkinson CT, Fleischer RC. 2004 Prevalence and differential host-specificity of two avian blood parasite genera in the Australo-Papuan region. *Mol. Ecol.* **13**, 3829–3844. (doi:10.1111/j.1365-294X.2004.02363.x)
- Beadell JS, Covas R, Gebhard C, Ishtiaq F, Melo M, Perkins SL, Graves GR, Fleischer RC. 2009 Host associations and evolutionary relationships of avian blood parasites from West Africa. *Int. J. Parasitol.* **39**, 257–266. (doi:10.1016/j.ijpara.2008.06.005)
- Latta SC, Ricklefs RE. 2010 Prevalence patterns of avian haemosporidia on Hispaniola. *J. Avian Biol.* **41**, 25–33. (doi:10.1111/j.1600-048X.2009.04685.x)

33. Ishtiaq F, Guillaumot L, Clegg SM, Phillimore AB, Black RA, Owens IPF, Mundy NI, Sheldon BC. 2008 Avian haematozoan parasites and their associations with mosquitoes across southwest Pacific Islands. *Mol. Ecol.* **17**, 4545–4555. (doi:10.1111/j.1365-294X.2008.03935.x)
34. Njabo KY, Cornel AJ, Sehgal RNM, Loiseau C, Buermann W, Harrigan RJ, Pollinger J, Valkiūnas G, Smith TB. 2009 *Coquillettidia* (Culicidae, Diptera) mosquitoes are natural vectors of avian malaria in Africa. *Malar. J.* **8**, 193. (doi:10.1186/1475-2875-8-193)
35. Njabo KY, Cornel AJ, Bonneaud C, Toffelmier E, Sehgal RNM, Valkiūnas G, Russell AF, Smith TB. 2011 Nonspecific patterns of vector, host and avian malaria parasite associations in a central African rainforest. *Mol. Ecol.* **20**, 1049–1061. (doi:10.1111/j.1365-294X.2010.04904.x)
36. Kimura M, Darbro JM, Harrington LC. 2010 Avian malaria parasites share congeneric mosquito vectors. *J. Parasitol.* **96**, 144–151. (doi:10.1645/GE-2060.1)
37. Kim KS, Tsuda Y. 2010 Seasonal changes in the feeding pattern of *Culex pipiens pallens* govern the transmission dynamics of multiple lineages of avian malaria parasites in Japanese wild bird community. *Mol. Ecol.* **19**, 5545–5554. (doi:10.1111/j.1365-294X.2010.04897.x)
38. Svensson-Coelho M, Ricklefs RE. 2011 Host phylogeography and beta diversity in avian haemosporidian (Plasmodiidae) assemblages of the Lesser Antilles. *J. Anim. Ecol.* **80**, 938–946. (doi:10.1111/j.1365-2656.2011.01837.x)
39. Wood MJ, Cosgrove CL, Wilkin TA, Knowles CL, Day KP, Sheldon BC. 2007 Within-population variation in prevalence and lineage distribution of avian malaria in blue tits, *Cyanistes caeruleus*. *Mol. Ecol.* **16**, 3263–3273. (doi:10.1111/j.1365-294X.2007.03362.x)
40. Kimura M, Dhondt AA, Lovette I. 2006 Phylogeographic structuring of *Plasmodium* lineages across the North American range of the house finch (*Carpodacus mexicanus*). *J. Parasitol.* **92**, 1043–1049. (doi:10.1645/GE-639R.1)
41. Ricklefs RE, Gray JD, Latta SC, Svensson-Coelho M. 2011 Distribution anomalies in avian haemosporidian parasites in the southern Lesser Antilles. *J. Avian Biol.* **42**, 570–584. (doi:10.1111/j.1600-048X.2011.05404.x)
42. Fallon SM, Ricklefs RE, Latta SC, Bermingham E. 2004 Temporal stability of insular avian malarial parasite communities. *Proc. R. Soc. Lond. B* **271**, 493–500. (doi:10.1098/rspb.2003.2621)
43. Ricklefs RE, Fallon SM. 2002 Diversification and host switching in avian malaria parasites. *Proc. R. Soc. Lond. B* **269**, 885–892. (doi:10.1098/rspb.2001.1940)
44. Ricklefs RE, Fallon SM, Bermingham E. 2004 Evolutionary relationships, cospeciation, and host switching in avian malaria parasites. *Syst. Biol.* **53**, 111–119. (doi:10.1080/10635150490264987)
45. Loss SR, Hamer GL, Walker ED, Ruiz MO, Goldberg TL, Kitron UD, Brawn JD. 2009 Avian host community structure and prevalence of West Nile virus in Chicago, Illinois. *Oecologia* **159**, 415–424. (doi:10.1007/s00442-008-1224-6)
46. Chaves LF, Hamer GL, Walker ED, Brown WM, Ruiz MO, Kitron UD. 2011 Climatic variability and landscape heterogeneity impact urban mosquito diversity and vector abundance and infection. *Ecosphere* **2**, article 70. (doi:10.1890/ES11-00088.1)
47. Huang S, Hamer GL, Molaei G, Walker ED, Goldberg TL, Kitron UD, Andreadis TG. 2009 Genetic variation associated with mammalian feeding in *Culex pipiens* from a West Nile virus epidemic region in Chicago, Illinois. *Vector Borne Zoonotic Dis.* **9**, 637–642. (doi:10.1089/vbz.2008.0146)
48. Fonseca DM, Keyghobadi N, Malcolm CA, Mehmet C, Schaffner F, Mogi M, Fleischer RC, Wilkerson RC. 2004 Emerging vectors in the *Culex pipiens* complex. *Science* **303**, 1535–1538. (doi:10.1126/science.1094247)
49. Fallon SM, Ricklefs RE, Swanson BL, Bermingham E. 2003 Detecting avian malaria: an improved polymerase chain reaction diagnostic. *J. Parasitol.* **89**, 1044–1047. (doi:10.1645/GE-3157)
50. Fecchio A, Lima MR, Svensson-Coelho M, Marini M<sup>Á</sup>, Ricklefs RE. 2013 Structure and organization of an avian haemosporidian assemblage in a Neotropical savanna in Brazil. *Parasitology* **140**, 181–192. (doi:10.1017/S0031182012001412)
51. Bensch S, Pérez-Tris J, Waldenström J, Hellgren O. 2004 Linkage between nuclear and mitochondrial DNA sequences in avian malaria parasites: multiple cases of cryptic speciation? *Evolution* **58**, 1617–1621.
52. Martinsen ES, Paperna I, Schall JJ. 2006 Morphological versus molecular identification of avian Haemosporidia: an exploration of three species concepts. *Parasitology* **133**, 279–288. (doi:10.1017/S0031182006000424)
53. Martinsen ES, Waite JL, Schall JJ. 2007 Morphologically defined subgenera of *Plasmodium* from avian hosts: test of monophyly by phylogenetic analysis of two mitochondrial genes. *Parasitology* **134**, 483–490. (doi:10.1017/S0031182006001922)
54. Harrington LC, Poulson RL. 2008 Considerations for accurate identification of adult *Culex restuans* (Diptera: Culicidae) in field studies. *J. Med. Entomol.* **45**, 1–8. (doi:10.1603/0022-2585(2008)45[1:CFAIOA]2.0.CO;2)
55. Crabtree MB, Savage HM, Miller BR. 1995 Development of a species-diagnostic polymerase chain reaction assay for the identification of *Culex* vectors of St Louis encephalitis virus based on interspecies sequence variation in ribosomal DNA spacers. *Am. J. Trop. Med. Hyg.* **53**, 105–109.
56. Biggerstaff BJ. 2012 *PooledInRate, version 4.0: a Microsoft add-in to compute prevalence estimates from pooled samples*. Fort Collins, CO: Centers of Disease Control and Prevention.
57. Guindon S, Gascuel O. 2003 A simple, fast, and accurate algorithm to estimate large phylogenies by maximum likelihood. *Syst. Biol.* **52**, 696–704. (doi:10.1080/10635150390235520)
58. Barker FK, Barrowclough GF, Groth JG. 2002 A phylogenetic hypothesis for passerine birds: taxonomic and biogeographic implications of an analysis of nuclear DNA sequence data. *Proc. R. Soc. Lond. B* **269**, 295–308. (doi:10.1098/rspb.2001.1883)
59. Wiersch SC, Maier WA, Kampen H. 2005 *Plasmodium* (Haemamoeba) *cathemerium* gene sequences for phylogenetic analysis of malaria parasites. *Parasitol. Res.* **96**, 90–94. (doi:10.1007/s00436-005-1324-8)
60. Valkiūnas G, Zehntindjiev P, Dimitrov D, Krizanauskienė A, Iezhova TA, Bensch S. 2008 Polymerase chain reaction-based identification of *Plasmodium* (Huffia) *elongatum*, with remarks on species identity of haemosporidian lineages deposited in GenBank. *Parasitol. Res.* **102**, 1185–1193. (doi:10.1007/s00436-008-0892-9)
61. Wilcox BR, Yabsley MJ, Ellis AE, Stallknecht DE, Gibbs SE. 2007 West Nile virus antibody prevalence in American crows (*Corvus brachyrhynchos*) and fish crows (*Corvus ossifragus*) in Georgia, USA. *Avian Dis.* **51**, 125–128. (doi:10.1637/0005-2086(2007)051[0125:WNVAPI]2.0.CO;2)
62. Westerdaal H, Waldenström J, Hansson B, Hasselquist D, von Schantz T, Bensch S. 2005 Associations between malaria and MHC genes in a migratory songbird. *Proc. R. Soc. B* **272**, 1511–1518. (doi:10.1098/rspb.2005.3113)
63. Bonneaud C, Perez-Tris J, Federici P, Chastel O, Sorci G. 2006 Major histocompatibility alleles associated with local resistance to malaria in a passerine. *Evolution* **60**, 383–389. (doi:10.1111/j.0014-3820.2006.tb01114.x)
64. Loiseau C, Zoorob R, Robert A, Chastel O, Julliard R, Sorci G. 2011 *Plasmodium relictum* infection and MHC diversity in the house sparrow (*Passer domesticus*). *Proc. R. Soc. B* **278**, 1264–1272. (doi:10.1098/rspb.2010.1968)
65. Cowman AF, Crabb BS. 2006 Invasion of red blood cells by malaria parasites. *Cell* **124**, 755–766. (doi:10.1016/j.cell.2006.02.006)
66. Hellgren O, Pérez-Tris J, Bensch S. 2009 A jack-of-all-trades and still a master of some: prevalence and host range in avian malaria and related blood parasites. *Ecology* **90**, 2840–2849. (doi:10.1890/08-1059.1)
67. LoGiudice K, Ostfeld RS, Schmidt KA, Keasing F. 2003 The ecology of infectious disease: effects of host diversity and community composition on Lyme disease risk. *Proc. Natl Acad. Sci. USA* **100**, 567–571. (doi:10.1073/pnas.0233733100)
68. Decaestecker E, Gaba S, Raeymaekers JA, Stoks R, Kerckhoven L, Ebert D, Meester L. 2007 Host–parasite ‘Red Queen’ dynamics archived in pond sediment. *Nature* **450**, 870–873. (doi:10.1038/nature06291)
69. Woodward BL *et al.* 2005 Host population persistence in the face of introduced vector-borne diseases: Hawaii amakihi and avian malaria. *Proc. Natl Acad. Sci. USA* **102**, 1531–1536. (doi:10.1073/pnas.0409454102)

**Electronic Supplementary Material for Medeiros *et al.* Host Compatibility Rather than the Vector-Host Encounter Rate Determines the Host Range of Avian *Plasmodium* Parasites**

**Section 1. Supplementary figures and data tables**

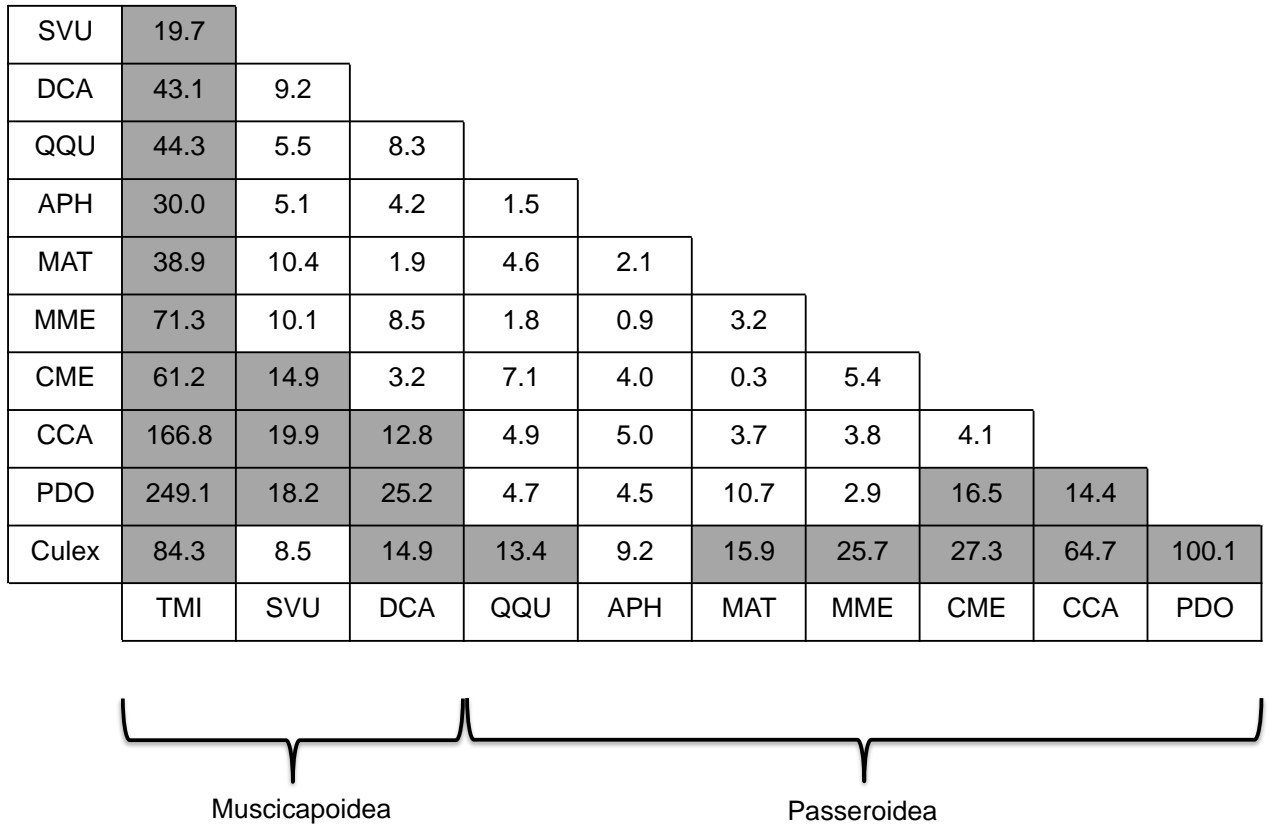


Figure S1. A grid summarising pairwise comparisons of parasite assemblages on avian hosts and the mosquito vectors in Chicago, IL, USA. The numbers within grid cells are G-statistics. Shaded grid cells denote statistically different comparisons ( $p < 0.05$ ; for all comparisons  $df=6$ ,  $G\text{-crit}=12.6$ ). The parasite community on *Turdus migratorius* (TMI) is distinct from all other hosts. Parasite communities on other hosts within Muscipoidea (DCA and SVU) are distinct from some communities on hosts within Passeroidea. Moreover, the parasite community within vectors is distinct from those in most hosts.

Table S1. Contingency table of *Culex* blood meals in Chicago, IL across the 10 common avian host species analysed. Whole digits represent the number of blood meals of an avian host species retrieved from a particular *Culex* species. The number within the parentheses represents the proportion of blood meals derived from a particular host species of the total number of blood meals for each *Culex* species.

	<i>Culex pipiens</i>	<i>Culex restuans</i>
<i>Agelaius phoeniceus</i>	2 (0.004)	4 (0.018)
<i>Cardinalis cardinalis</i>	42 (0.090)	25 (0.110)
<i>Carpodacus mexicanus</i>	37 (0.079)	8 (0.035)
<i>Dumetella carolinensis</i>	2 (0.004)	2 (0.009)
<i>Melospiza melodia</i>	2 (0.004)	1 (0.004)
<i>Molothrus ater</i>	0	2 (0.009)
<i>Passer domesticus</i>	77 (0.165)	37 (0.163)
<i>Quiscalus quiscula</i>	3 (0.006)	2 (0.009)
<i>Sturnus vulgaris</i>	12 (0.026)	12 (0.053)
<i>Turdus migratorius</i>	289 (0.620)	134 (0.590)

## Section 2. Recombination activating gene 1 (RAG1) phylogeny

Phylogenetic distances among hosts were estimated by sequencing and aligning a 656-bp fragment of the recombination activating gene 1 (RAG1). RAG-1 was amplified with primers RAG-1F (5'GCA AKA ATA YAC ATC TCA GYACCA MG 3') and RAG-1R (5' GCT GYA TCA TAT CGR AAT CTC TTY GC 3'). PCR reactions consisted of 1X buffer, 200 nM of each dNTP, 2 mM MgCl<sub>2</sub>, 0.02% BSA, 200 nM of each primer, and 0.5 units of TaKaRa Taq<sup>TM</sup> (TaKaRa Bio Inc., Shiga, Japan). The PCR involved an initial denaturing period at 94°C for 4 min, 35 cycles of 94°C for 30 s, 55°C for 30 s, 72°C for 1 min, and a final extension step at 72°C for 3 min. A maximum likelihood gene tree was constructed with a GTR +  $\gamma$  model (gamma=0.23) using the PHYML plug-in in the program Geneious. *Gallus gallus* (AF143730), *Meliphaga analoga* (AY057003), and *Formicarius colma* (AY056993) were included as outgroups.

GenBank accession numbers for RAG-1 sequences of all hosts are as follows: TMI (KC789829), MAT (KC789831), QQU (KC789830), SVU (AY057032), DCA (AY319981), CME (EU165349), PDO (EF568263), CCA (AY056982), APH (KC789833), and MME(KC789832). Patristic distances were extracted from the tree and used in subsequent analyses (Table S2).

Table S2. Table of the patristic distances of hosts based on a maximum likelihood analysis of a 656-bp fragment of the recombination-activating gene 1 (RAG1). The species abbreviation code includes the first letter of the genus name and the first two letters of the species name.

	TMI	MAT	QQU	SVU	DCA	CME	PDO	CCA	APH
MAT	0.071								
QQU	0.070	0.014							
SVU	0.039	0.062	0.060						
DCA	0.041	0.068	0.067	0.036					
CME	0.059	0.035	0.033	0.050	0.056				
PDO	0.054	0.037	0.035	0.045	0.051	0.024			
CCA	0.064	0.036	0.034	0.055	0.061	0.027	0.029		
APH	0.067	0.011	0.006	0.057	0.064	0.030	0.032	0.031	
MME	0.063	0.034	0.034	0.054	0.060	0.027	0.029	0.018	0.030

### Section 3. Monte Carlo simulation of parasite distributions across hosts

*Set 1. Monte Carlo simulations of the distribution of Plasmodium parasites across avian hosts based on their cumulative frequency in the sample.*

For each run of this simulation, host individuals of a given species were assigned to *Plasmodium* infections based on the proportion of a specific *Plasmodium* lineage in the sample (Table 1). The original number of infections per host species was maintained in each run of the simulation. 100,000 runs were performed. This procedure was repeated for each host species.

Table S3a summarises the results. The actual number of infections for 24 of 70 possible host-parasite combinations was outside the 5% confidence limits of the simulated distribution. CHI09PL, *Agelaius phoeniceus*, and *Sturnus vulgaris* did not demonstrate any deviations from the expected number of infections. In general, the parasite lineages CHI02PL and CHI07PL were less abundant than expected on hosts within the superfamily Passeroidea. This was especially apparent for the well-sampled *Passer domesticus* and *Cardinalis cardinalis*, and for the CHI07PL across many hosts. In addition, CHI02PL, CHI04PL, and CHI07PL were more abundant on *Turdus migratorius* than expected. *P. cathermerium* and *P. elongatum*, showed the opposite pattern, being overly abundant across many Passeroidea hosts and nearly absent on *Turdus migratorius*. CHI05PL was overly abundant on *Passer domesticus*, and less abundant on *Turdus migratorius*.

This analysis generally demonstrates how the distribution of *Plasmodium* parasites across host species analysed here differs from random expectations based on the frequency in which both parasites and host species were sampled.

*Set 2. Monte Carlo simulations of the distribution of parasites across hosts based on the actual proportion of parasites in Culex mosquito vectors.*

For each run of this simulation, host individuals of a given species were assigned to *Plasmodium* lineages based on the proportion of the *Plasmodium* lineage within the sample of infected vectors (Table 1). The original number of infections per host species was maintained in each run of the simulation. 100,000 runs were performed. This procedure was repeated for each host species.

Table S3b summarises the results. The actual number of infections for 31 of 70 possible host-parasite combinations was outside the 5% confidence limits of the simulated distribution. *Agelaius phoeniceus* did not demonstrate any deviations from expected number of infections. General patterns were similar to Set 1, with CHI02PL, and CHI07PL being more common on *T. migratorius* and less common of Passeroidea hosts, and *P. elongatum*, *P. cathemerium*, and CHI05PL being less common on *T. migratorius* and more common of Passeroidea hosts. Interestingly, most hosts had fewer CHI04PL infections than expected. This is associated with an unexpectedly high proportion of CHI04PL infections in *Culex* vectors.

If the two species of *Culex* vectors feed on hosts at equivalent rates, each parasite has the same relative access to hosts independent of its vector. Assuming that host compatibility issues were not present, this would suggest that hosts and vectors would have the same relative proportions of each parasite. Both this simulation and the G-test comparing the parasite assemblage in vectors to those of specific host species (Figure S1) show this is not the case. The results suggest that a strong host compatibility filter restricts the distribution of parasites across hosts. Unlike the G-test however, this approach provides a statistically explicit way of identifying host-parasite pairs that depart from random. Once again, this simulation highlights the lack of *P. elongatum* and *P. cathemerium* infections in *T. migratorius*.

*Set 3. Monte Carlo simulations of the distribution of Plasmodium parasites across hosts based on the frequency of the parasites and mosquito vector-feeding probabilities on each host.*

For each run of this simulation, *Plasmodium* infections were assigned to hosts of a given species based on the proportion of *Culex* blood meals derived from that species. Here, the proportion of blood meals is assumed to represent the probability that an infectious mosquito will bite a particular host species. Because both *Culex* species had statistically indistinguishable feeding patterns, they were combined to estimate this probability. The original number of infections of each parasite lineage in the sample was maintained in each run of the simulation. 100,000 runs were performed. This procedure was repeated for each *Plasmodium* lineage.

Because this procedure assigns *Plasmodium* lineages to hosts based on the feeding probabilities of vectors, it does not explicitly account for host abundance. Instead, we assume that the prevalence of each lineage is constant across the simulation and the actual sample. Thus, the expected values and the confidence limits generated by the simulation express the number of parasites of a specific lineage that should be recovered from each host species given that 1) the same number of birds (N=1596) were resampled and 2) mosquito biting probabilities determine *Plasmodium* host range. Therefore, the actual number of infections per host species is only comparable to these expected values and their confidence limits if host species were sampled commensurate to their relative abundance and availability to host-seeking mosquitoes. We use both point counts with distance sampling and mist-netting capture data to estimate the relative abundance of each species in the community (Table S3c). A description of the methods on the point count surveys can be found in Hamer *et al.* [14]. The relative abundance of bird populations can be difficult to estimate as different techniques have inherent biases. Ground-level mist-nets may vary in their ability to capture birds of

different sizes, and may be biased against those that occupy the canopy (although the relatively minor vertical stratification of urban-suburban habitat makes this less of a concern for our study). Point counts may miss individuals of cryptic species that are less conspicuous. Thus, we averaged the relative proportions of each species across both methods to mitigate the inherent biases of each technique by itself.

The proportion of each species in the actual sample was highly correlated with the average proportion of each in the community (Figure S2,  $R^2=0.89$ ,  $p<0.0001$ ). However, the slope of the regression line (0.71) demonstrated that the values of each proportion were not equal. Therefore, we rescaled the results of the initial simulation (summarized in Table S3d) by converting the expected confidence limits and the actual values into prevalence. We divide the expected confidence limits by the number of individuals of each species that should exist in a community of 1596 birds sampled without bias (ie. the average proportion of a species in the community \* 1596). We divide the actual values by the actual number of individuals sampled per host species. Rescaled values are summarized in Table S3e.

This simulation attempts to control for a mosquito-imposed encounter rate. Thus, cases in which observed values deviate from the range of expected values might highlight specific cases in which a host compatibility filter is operating. This simulation is slightly more conservative than others presented here. The prevalences of 22 of 70 possible host-parasite combinations were outside the 5% confidence limits of the simulated distribution. However, the same major pattern evident throughout our analysis maintains. CHI07PL, CHI02PL, and CHI04PL (though marginally so for the later) are more prevalent on *T. migratorius* than expected, while CHI05PL, *P.*

*cathemerium*, and *P. elongatum* are less prevalent on *T. migratorius* than expected. The prevalences of *P. cathemerium*, and *P. elongatum* are equal to or exceed the expected prevalences on most Passeroidea hosts (although *C. mexicanus* and *P. cathemerium* is an interesting exception). CHI07PL and CHI02PL are nearly absent from Passeroidea host, and are less prevalent on well-sampled Passeroidea hosts than expected. CHI05PL is more prevalent on 3 Passeroidea hosts than expected, most notably on *P. domesticus*.

Table S3a. Results of Monte Carlo simulations (Set 1) of the distribution of *Plasmodium* parasites across avian hosts based their cumulative frequency in the sample. EV is the expected value and represents the mean simulated value across the 100,000 runs. CL shows the 95% confidence limits based on the 100,000 runs in the simulation. AV is the actual number of infections observed. Highlighted cells represent host-parasite pairs in which the actual value of infections lies outside the 95% confidence limits of the simulation. Abbreviations for host species include the first letter of the genus, and the first two letters of the species name respectively.

	CHI02PL			CHI04PL			CHI07PL			CHI09PL			P.CATH			P.ELON			CHI05PL		
	EV	CL	AV	EV	CL	AV	EV	CL	AV	EV	CL	AV	EV	CL	AV	EV	CL	AV	EV	CL	AV
<b>APH</b>	0.52	0,2	0	0.37	0,2	0	2.31	0,5	0	0.15	0,1	0	1.99	0,4	4	1.25	0,3	2	0.42	0,2	1
<b>CCA</b>	3.84	1,8	0	2.75	0,6	0	17.16	11,24	0	1.11	0,4	0	14.74	9,21	26	9.33	4,15	24	3.07	0,7	2
<b>CME</b>	1.18	0,4	0	0.85	0,3	0	5.29	2,9	0	0.34	0,2	0	4.53	1,8	4	2.88	0,6	12	0.95	0,3	0
<b>DCA</b>	1.49	0,4	0	1.06	0,3	2	6.60	3,11	4	0.42	0,2	0	5.66	2,10	4	3.59	1,7	10	1.18	0,4	0
<b>MAT</b>	0.74	0,3	0	0.53	0,2	0	3.30	1,6	0	0.21	0,1	0	2.83	0,6	3	1.79	0,4	7	0.60	0,2	0
<b>MME</b>	1.49	0,4	0	1.06	0,3	0	6.59	3,11	0	0.42	0,2	0	5.67	2,10	11	3.60	1,7	6	1.19	0,4	3
<b>PDO</b>	7.12	3,13	0	5.07	1,10	0	31.65	23,41	2	2.03	0,5	1	27.22	19,36	56	17.22	10,25	17	5.68	2,11	20
<b>SVU</b>	0.96	0,3	0	0.69	0,3	0	4.28	1,8	6	0.28	0,2	0	3.69	1,7	7	2.34	0,5	0	0.77	0,3	0
<b>TMI</b>	16.81	10,25	35	11.98	6,19	23	74.88	61,89	144	4.79	1,9	9	64.32	51,78	9	40.77	30,52	5	13.46	7,21	2
<b>QQU</b>	0.89	0,3	0	0.64	0,2	0	3.95	1,7	0	0.25	0,2	0	3.41	1,7	10	2.15	0,5	2	0.70	0,3	0

Table S3b. Results of Monte Carlo simulations (Set 2) of the distribution of parasites across hosts based on the actual proportion of parasites in *Culex* mosquito vectors. EV is the expected value and represents the mean simulated value across the 100,000 runs. CL shows the 95% confidence limits based on the 100,000 runs in the simulation. AV is the actual number of infections observed. Highlighted cells represent host-parasite pairs in which the actual value of infections lies outside the 95% confidence limits of the simulation. Abbreviations for host species include the first letter of the genus, and the first two letters of the species name respectively.

	CHI02PL			CHI04PL			CHI07PL			CHI09PL			P.CATH			P.ELON			CHI05PL		
	EV	CL	AV	EV	CL	AV	EV	CL	AV	EV	CL	AV	EV	CL	AV	EV	CL	AV	EV	CL	AV
<b>APH</b>	0.76	0,3	0	2.02	0,4	0	1.59	0,4	0	0.11	0,1	0	1.75	0,4	4	0.65	0,2	2	0.11	0,1	1
<b>CCA</b>	5.69	2,10	0	15.03	9,22	0	11.78	6,18	0	0.81	0,3	0	13.01	7,19	26	4.88	1,9	24	0.81	0,3	2
<b>CME</b>	1.75	0,4	0	4.62	1,8	0	3.64	1,7	0	0.25	0,2	0	4.00	1,8	4	1.50	0,4	12	0.25	0,2	0
<b>DCA</b>	2.18	0,5	0	5.79	2,10	2	4.53	1,8	4	0.31	0,2	0	5.00	2,9	4	1.88	0,5	10	0.31	0,2	0
<b>MAT</b>	1.10	0,3	0	2.89	0,5	0	2.27	0,5	0	0.16	0,1	0	2.50	0,5	3	0.94	0,3	7	0.16	0,1	0
<b>MME</b>	2.19	0,5	0	5.78	2,10	0	4.53	1,8	0	0.31	0,2	0	5.00	2,9	11	1.87	0,5	6	0.31	0,2	3
<b>PDO</b>	10.50	5,17	0	27.72	19,37	0	21.76	14,30	2	1.50	0,4	1	24.01	16,33	56	9.00	4,15	17	1.50	0,4	20
<b>SVU</b>	1.42	0,4	0	3.76	1,7	0	2.94	0,6	6	0.20	0,1	0	3.26	1,6	7	1.22	0,4	0	0.20	0,1	0
<b>TMI</b>	24.83	16,34	35	65.60	52,79	23	51.45	39,64	144	3.55	0,8	9	56.78	44,70	9	21.26	13,30	5	3.55	0,8	2
<b>QQU</b>	1.31	0,4	0	3.47	1,7	0	2.73	0,6	0	0.19	0,1	0	3.00	0,6	10	1.12	0,3	2	0.19	0,1	0

Table S3c. Table demonstrating the number of individuals sampled and screened for *Plasmodium* parasites, the proportion of this sample, and the proportion in the avian community as measured through point surveys with distance sampling methods (Hamer et al. [14]) and mist-net captures for each host species.

Host Species	Number Sampled	Proportion of the sample	Proportion in community (point counts)	Proportion in community (net captures)
APH	55	0.034	0.054	0.036
CCA	122	0.076	0.017	0.064
CME	79	0.049	0.013	0.032
DCA	151	0.095	0.006	0.092
MAT	20	0.013	0.003	0.013
MME	72	0.045	0.002	0.044
PDO	545	0.341	0.526	0.452
SVU	66	0.041	0.068	0.028
TMI	435	0.273	0.242	0.219
QQU	51	0.032	0.069	0.020
Sum	1596	1	1	1

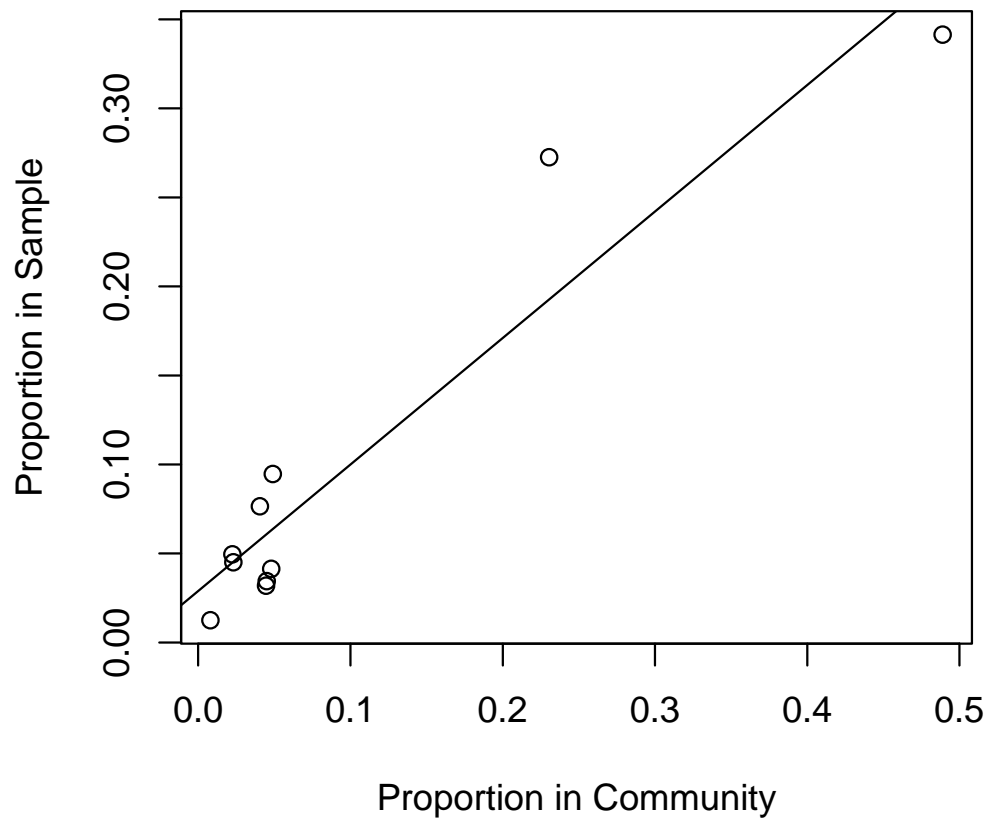


Figure S2. Plot of the proportion of a host species in the sample regressed against the estimated proportion in the community. The community proportion is estimated by averaging host species proportions based on point counts and mist net captures (see Table 3c).

Table S3d. Results of Monte Carlo simulations (Set 3) of the distribution of parasites across hosts based on the frequency of the parasites and mosquito vector-feeding probabilities on each host. EV is the expected value and represents the mean simulated value across the 100,000 runs. CL shows the 95% confidence limits based on the 100,000 runs in the simulation. AV is the actual number of infections observed. Abbreviations for host species include the first letter of the genus, and the first two letters of the species name respectively.

		<u>CHI02PL</u>	<u>CHI04PL</u>	<u>CHI07PL</u>	<u>CHI09PL</u>	<u>P.CATH</u>	<u>P.ELON</u>	<u>CHI05PL</u>
<b>APH</b>	EV	0.31	0.22	1.35	0.09	1.16	0.74	0.24
	CL	0,2	0,1	0,4	0,1	0,4	0,3	0,1
	AV	0	0	0	0	4	2	1
<b>CCA</b>	EV	3.39	2.41	15.08	0.97	12.94	8.22	2.7
	CL	0,7	0,6	8,23	0,3	7,20	3,14	0,6
	AV	0	0	0	0	26	24	2
<b>CME</b>	EV	2.28	1.63	10.12	0.65	8.7	5.52	1.82
	CL	0,5	0,4	5,16	0,2	4,15	2,10	0,5
	AV	0	0	0	0	4	12	0
<b>DCA</b>	EV	0.20	0.14	0.9	0.06	0.78	0.49	0.16
	CL	0,1	0,1	0,2	0,1	0,3	0,2	0,1
	AV	0	2	4	0	4	10	0
<b>MAT</b>	EV	0.10	0.07	0.45	0.03	0.39	0.24	0.08
	CL	0,1	0,1	0,2	0,1	0,2	0,2	0,1
	AV	0	0	0	0	3	7	0
<b>MME</b>	EV	0.15	0.11	0.67	0.04	0.58	0.37	0.12
	CL	0,1	0,1	0,3	0,1	0,2	0,2	0,1
	AV	0	0	0	0	11	6	3
<b>PDO</b>	EV	5.76	4.11	25.66	1.64	22.04	13.99	4.61
	CL	2,10	1,8	17,35	0,4	14,31	8,21	1,9
	AV	0	0	2	1	56	17	20
<b>SVU</b>	EV	1.21	0.86	5.41	0.35	4.64	2.95	0.97
	CL	0,4	0,3	1,10	0,2	1,9	0,7	0,3
	AV	0	0	6	0	7	0	0
<b>TMI</b>	EV	21.35	15.27	95.24	6.1	81.82	51.87	17.09
	CL	16,27	10,20	83,107	3,9	71,93	43,61	12,22
	AV	35	23	144	9	9	5	2
<b>QQU</b>	EV	0.25	0.18	1.13	0.07	0.96	0.62	0.2
	CL	0,2	0,1	0,4	0,1	0,3	0,2	0,1
	AV	0	0	0	0	10	2	0

Table S3e. Rescaled lower and upper 95% confidence limits (LCL/UCL, respectively) from Set 3 of the Monte Carlo simulations. Confidence limits and the actual values are rescaled by dividing the expected number of individuals per host species (average proportion of the species in the community \* 1598) and the number of host actually sampled per species, respectively (see Tables S3c & S3d). Thus, cell values represent rescaled prevalences to mitigate bias in sampling effort. Host identities are in the upper-left corner for each sub-table.

<b>APH</b>	rescaled LCL	rescaled UCL	rescaled AV	<b>CCA</b>	rescaled LCL	rescaled UCL	rescaled AV
CHI02PL	0.000	0.028	0.000	CHI02PL	0.000	0.108	0.000
CHI04PL	0.000	0.014	0.000	CHI04PL	0.000	0.093	0.000
CHI07PL	0.000	0.056	0.000	CHI07PL	0.124	0.356	0.000
CHI09PL	0.000	0.014	0.000	CHI09PL	0.000	0.046	0.000
P.CATH	0.000	0.056	0.073	P.CATH	0.108	0.309	0.213
P.ELON	0.000	0.042	0.036	P.ELON	0.046	0.217	0.197
CHI05PL	0.000	0.014	0.018	CHI05PL	0.000	0.093	0.016

<b>CME</b>	rescaled LCL	rescaled UCL	rescaled AV	<b>DCA</b>	rescaled LCL	rescaled UCL	rescaled AV
CHI02PL	0.000	0.139	0.000	CHI02PL	0.000	0.013	0.000
CHI04PL	0.000	0.111	0.000	CHI04PL	0.000	0.013	0.013
CHI07PL	0.139	0.446	0.000	CHI07PL	0.000	0.026	0.026
CHI09PL	0.000	0.056	0.000	CHI09PL	0.000	0.013	0.000
P.CATH	0.111	0.418	0.051	P.CATH	0.000	0.038	0.026
P.ELON	0.056	0.278	0.152	P.ELON	0.000	0.026	0.066
CHI05PL	0.000	0.139	0.000	CHI05PL	0.000	0.013	0.000

<b>MAT</b>	rescaled LCL	rescaled UCL	rescaled AV	<b>MME</b>	rescaled LCL	rescaled UCL	rescaled AV
CHI02PL	0.000	0.078	0.000	CHI02PL	0.000	0.027	0.000
CHI04PL	0.000	0.078	0.000	CHI04PL	0.000	0.027	0.000
CHI07PL	0.000	0.157	0.000	CHI07PL	0.000	0.082	0.000
CHI09PL	0.000	0.078	0.000	CHI09PL	0.000	0.027	0.000
P.CATH	0.000	0.157	0.150	P.CATH	0.000	0.054	0.153
P.ELON	0.000	0.157	0.350	P.ELON	0.000	0.054	0.083
CHI05PL	0.000	0.078	0.000	CHI05PL	0.000	0.027	0.042

<b>PDO</b>	rescaled LCL	rescaled UCL	rescaled AV	<b>SVU</b>	rescaled LCL	rescaled UCL	rescaled AV
CHI02PL	0.003	0.013	0.000	CHI02PL	0.000	0.052	0.000
CHI04PL	0.001	0.010	0.000	CHI04PL	0.000	0.039	0.000
CHI07PL	0.022	0.045	0.004	CHI07PL	0.013	0.131	0.091
CHI09PL	0.000	0.005	0.002	CHI09PL	0.000	0.026	0.000
P.CATH	0.018	0.040	0.103	P.CATH	0.013	0.117	0.106
P.ELON	0.010	0.027	0.031	P.ELON	0.000	0.091	0.000
CHI05PL	0.001	0.012	0.037	CHI05PL	0.000	0.039	0.000

<b>TMI</b>	rescaled LCL	rescaled UCL	rescaled AV	<b>QQU</b>	rescaled LCL	rescaled UCL	rescaled AV
CHI02PL	0.043	0.073	0.080	CHI02PL	0.000	0.028	0.000
CHI04PL	0.027	0.054	0.053	CHI04PL	0.000	0.014	0.000
CHI07PL	0.226	0.291	0.331	CHI07PL	0.000	0.056	0.000
CHI09PL	0.008	0.024	0.021	CHI09PL	0.000	0.014	0.000
P.CATH	0.193	0.253	0.021	P.CATH	0.000	0.042	0.196
P.ELON	0.117	0.166	0.011	P.ELON	0.000	0.028	0.039
CHI05PL	0.033	0.060	0.005	CHI05PL	0.000	0.014	0.000

#### Section 4. Does host age influence the patterns observed here?

Parasites can be heterogeneously distributed across age classes. Hosts of different ages have variable levels of exposure, with older hosts having an increase exposure often to a wider range of parasites. Moreover, in the case of avian malaria parasites, infections acquired early in life may remain chronic for long-periods of time, even for the duration of the host's life [25]. Here, we ask whether heterogeneity in parasite-host interactions exists across age classes and influences some of the patterns we report.

The main dataset (presented in Table 1) was divided across two host age classes: hatch year birds (HY), which have only been exposed to one transmission season, and after hatch-year birds (AHY), which have been exposed to more than one transmission season. The resulting datasets are presented in Tables S4a-b. The structure of distance matrices that summarise beta-similarities in the parasite assemblages among hosts of AHY and HY birds were compared by a Mantel test with 10,000 permutations. *Agelaius phoeniceus* was excluded from this analysis because only two HY individuals were sampled and neither had a *Plasmodium* infection. The two matrices were highly correlated (Mantel  $r = 0.71$ ,  $p=0.0001$ ) suggesting that differences in the parasite interactions among species are similar between AHY and HY individuals. The same set of Mantel tests presented in the main text was performed on the distance matrices composed of either AHY or HY birds. Beta similarities in the relationship with *Plasmodium* lineages and avian *Plasmodium* vectors across avian hosts were not correlated for both AHY and HY birds (Mantel  $r = -0.22$ ,  $-0.09$ ,  $p=0.88$ ,  $0.60$ ; respectively). However, beta-similarities in *Plasmodium* relationships were correlated with phylogenetic similarity (Mantel  $r = 0.55$ ,  $0.46$ ,  $p=0.026$ ,  $0.017$ ; respectively). Age does not appear to influence the main patterns presented here, namely that 1) relationships with

mosquitoes do not limit the distribution of parasites across hosts and 2) phylogenetically related hosts have more similar relationships with parasites.

Table S4a. Number of *Plasmodium* infections of specific lineages across hatch-year (juvenile) individuals of all 10 avian hosts. Abbreviations for host species include the first letter of the genus, and the first two letters of the species name respectively.

*Plasmodium* Parasites

Hosts								
	CHI02PL	CHI04PL	CHI07PL	CHI09PL	P.CATH	P.ELON	CHI05PL	TOTAL
CCA	0	0	0	0	16	15	1	32
CME*	0	0	0	0	2	7	0	9
DCA	0	2	2	0	2	4	0	10
MAT*	0	0	0	0	1	3	0	4
MME	0	0	0	0	3	4	3	10
PDO	0	0	1	0	34	8	7	50
SVU	0	0	2	0	6	0	0	8
TMI	8	15	43	6	9	4	1	86
QQU	0	0	0	0	5	1	0	6
TOTAL	8	17	48	6	78	46	12	

Table S4b. Number of *Plasmodium* infections of specific lineages across after hatch-year (adult) individuals of all 10 avian hosts. Abbreviations for host species include the first letter of the genus, and the first two letters of the species name respectively.

*Plasmodium* Parasites

Hosts								
	CHI02PL	CHI04PL	CHI07PL	CHI09PL	P.CATH	P.ELON	CHI05PL	TOTAL
CCA	0	0	0	0	10	9	1	20
CME*	0	0	0	0	1	5	0	6
DCA	0	0	2	0	2	6	0	10
MAT*	0	0	0	0	2	3	0	5
MME	0	0	0	0	8	2	0	10
PDO	0	0	1	1	22	9	13	46
SVU	0	0	4	0	1	0	0	5
TMI	27	8	101	3	0	1	1	141
QQU	0	0	0	0	5	1	0	6
TOTAL	27	8	108	4	51	36	15	

\* CME and MAT does not sum to 16 and 10 across the AHY and HY tables as presented in Table 1 because 1 infected individual was not reliably aged for both species